JOURNAL OF MATERIALS SCIENCE 30 (1995) 1273–1276

Structure and electrical properties of vacuum-deposited antimony telluride thin films on an amorphous substrate

Z. S. EL MANDOUH
National Research Centre, Dokki, Cairo, Egypt

Sb_2Te_3 thin films, 50–109 nm thick, have been prepared by vacuum evaporation on to quartz substrates. Electrical properties of as-deposited and annealed films show that the activation energy is thickness dependent. Optical measurements indicate that there is an indirect transition having an energy of 1.9 eV. Transmission electron micrographs show the fine grains of the deposit.

1. Introduction

Sb_2Te_3 crystal ranks among the family of layer-structure semiconductors having the space group D_{3d}^5–R 3*m*. The use of Sb_2Te_3 in the field of thermoelectrical applications calls for the preparation of single or polycrystalline materials with well-defined transport properties.

The bulk $Bi_{1-x}Sb_x$ alloy system has been studied by Tichovolsky and Mavroides [1], and Esaki and Stiles [2] observed semiconducting behaviour in the *x* range 0.07 to about 0.22. Many studies [3] have also been made on the structure and electrical properties of thin alloy films. Dass and Lakshmi [4] observed semiconducting behaviour in thin films of $Sb_{50}Te_{50}$ alloy after the first annealing cycle. In addition, when the film was annealed, they observed the transition from the amorphous to the crystalline state. So far, no work has been performed on thin films of Sb–Te alloy. The crystal lattice of Sb_2Te_3 is formed by a periodic arrangement of layers oriented perpendicular to the trigonal axis, *c*. Each layer is composed of five atomic planes arranged according to the following pattern:

$$\mathrm{Te^1Sb\ Te^{11}Sb\ Te^1 \cdots Te^1Sb\ Te^{11}Sb\ Te^1 \cdots}$$

Every Te^{11} atom is octahedrally surrounded by six antimony atoms. Octahedral coordination is exhibited also by the antimony atoms ($3Te^1$ atoms from one side and $3Te^{11}$ from other side) as well as Te^1 atoms (3Sb atoms from one side and $3Te^1$ atoms of the neighbouring layer) stack from the other side [5].

2. Experimental procedure

The starting material for the growth experiments was prepared by mixing the pure elements of antimony and tellurium stoichometrically in a sealed silica ampoule evacuated to a pressure of about 10^{-4} torr (1 torr = 133.322 Pa) to prepare Sb_2Te_3. The ampoule was heated at about 973 K for 18 h.

An X-ray diffractometer (Philips D500), using monochromatic CuK_α radiation, was employed to obtain diffraction patterns from films deposited on quartz substrates. A wide range of 2 θ (from 16°–90°) was scanned so that all possible diffraction peaks could be detected. Films intended for electrical and optical measurements were deposited on quartz substrates.

3. Results and discussion

When X-rays encounter any form of matter they are partly transmitted and partly absorbed. Experiments shows that the fractional decrease in intensity, *I*, of an X-ray beam as it passes through any homogeneous substance is proportional to the distance traversed, *x*. In differential form

$$\frac{-\,\mathrm{d}I}{I} = \alpha\,\mathrm{d}x \tag{1}$$

where the proportionality constant, α, is called the linear absorption coefficient and is dependent on the substance considered, its density, and the wavelength of the X-rays. Integration gives:

$$I_x = I_0 e^{-\alpha x} \tag{2}$$

where I_0 is the intensity of the incident X-ray beam and I_x the intensity of transmitted beam after passing through a thickness *x*.

A typical X-ray diffraction (XRD) pattern for thin films of Sb_2Te_3 deposited in a vacuum is shown in Fig. 1a which indicates that only the characteristic peak of Sb_2Te_3 $d = 3.15$ and a small peak are observed for as-deposited films of Sb_2Te_3. Annealing of films after deposition has a pronounced effect on the crystallinity and composition of the film. Annealing at 473 K improves crystallinity of the films (Fig. 1b) where the XRD lines become sharper and the characteristic lines of triganol Sb_2Te_3 become very prominent. It can also be seen that the grain size increases in this case, as indicated by the decreasing half

0022–2461

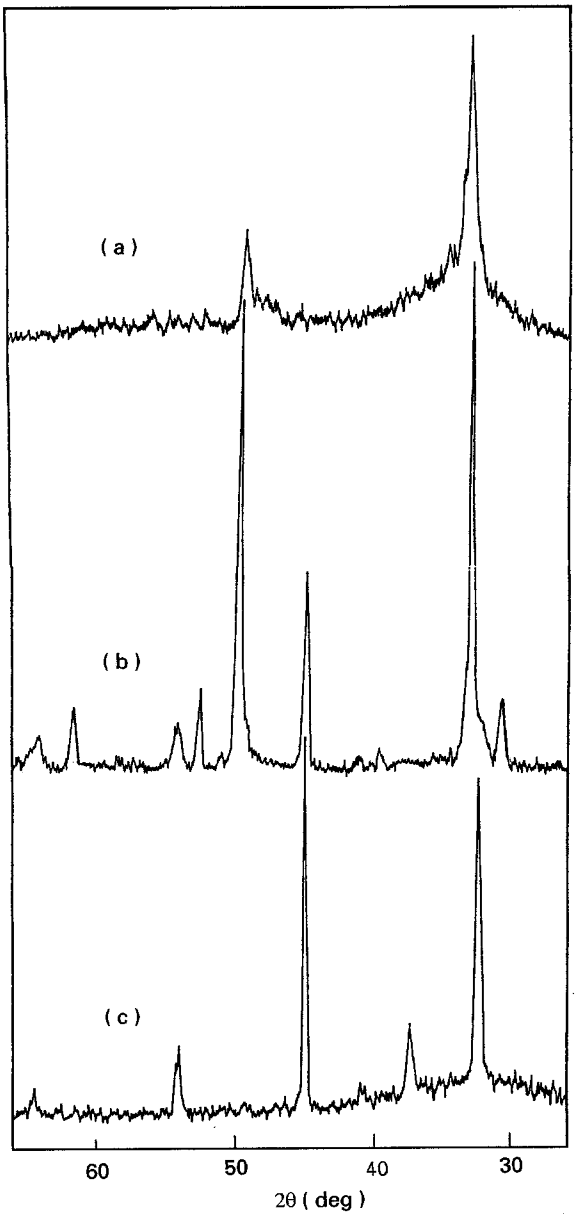

Figure 1 X-ray diffraction patterns of Sb_2Te_3 at different annealing temperatures: (a) thin-film Sb_2Te_3, (b) thin film annealed at 473 K, (c) thin film annealed at 573 K.

TABLE I X-ray diffraction lines of thin films of Sb_2Te_3 annealed at different temperatures

d-spacing of as-deposited film	*hkl*	473 K	*hkl*	573 K
		3.38	009	
3.15	015	3.15[a]	015	
		2.64	018	
		2.34	$101\underline{0}$	2.3435
2.13	110	2.13	110	
		2.0308	$001\underline{5}$	
		1.9714	1013	1.97
		1.765	205	
		$1.68\underline{8}$	$001\underline{8}$	1.6889

[a] Characteristic peak (100% Sb_2Te_3).

line width of the X-ray reflections. On prolonged annealing to higher temperature, 573 K, the film began to dissociate, as is evident from Fig. 1c, and the characteristic peak ($d = 3.15$) disappears. Dissociation of the film may be attributed to the escape of tellurium from the film [6]. These results indicate that for obtaining monophasic film, the annealing time must be decreased and the annealing temperature must not exceed 473 K.

The results for the X-ray spectrum of Sb_2Te_3 at different annealing temperatures are shown in Table I.

The sheet resistance of metallic thin films decreases by several orders of magnitude as the film structure changes from the discontinuous to the uniform continuous film structure. Similarly, there is a pronounced change in the optical absorption spectrum. The resistivity of discontinuous films is high and is governed by quantum tunnelling. The resulting high sheet resistance is attractive for applications in electronic microcircuits. Electrical conduction in a solid results from the movement of current carriers, either electrons or ions, or possibly both, through the material.

In the case of a discontinuous film, the conducting properties are a highly complicated problem. An analysis of the temperature dependence of conductivity brings in additional difficulties, e.g. from the variation in particle separation due to the change of dimensions of the substrate with temperature. Thus the temperature dependence of conductivity will depend on:

(a) the change in conductance of individual particles;

(b) changes in tunnelling probability due to variation in crystallite separation;

(c) Variation in conducting properties of the substrate with temperature, and

(d) Annealing effects in particle or substrate.

If the separation between particles is increased, the probability of tunnelling will decrease. For large particles separated by gaps small enough to give a high quantum mechanical tunnelling probability, the overall film resistivity will be determined by the resistance of the individual particles. This will, in turn, be governed by the particle dimensions in relation to the electron mean-free path and the influence of defects [7].

Fig. 2 shows log ρ versus temperature plots during heating of the films of different thicknesses. Immediately after deposition, it can be seen that there is an abrupt fall in resistance of the films between 385 and 312 K, while there is no such sharp decrease during cooling. This indicates that the films undergo an irreversible transition on heating. This behaviour has been observed on Se–Te alloy films [4].

Our present work on the conductivity of Sb_2Te_3 films mainly deals with the analysis of the temperature and thickness dependence of conductivity of both as-deposited and exposed films. The resistivity of Sb_2Te_3 films was measured at room temperature and up to 473 K and this is consistent with the phase and structural changes occurring to the film as observed in the X-ray diffraction spectrum above such a temperature. Fig. 3 illustrates the temperature variation of resistivity, log ρ, against $1/T$ for annealed Sb_2Te_3 thin films of different thicknesses ranging from 50–109 nm stoichiometric films. It was found that the relation between log ρ and $1/T$ for annealed films was linear for all thicknesses [8].

These results indicate an activated conduction and semiconducting nature of the film. The activation energy was calculated by equating the slopes of resistivity curves by $\Delta E/KT$. The calculated values were extrapolated from 0.016 eV to 0.073 eV. The thickness has a pronounced effect on the conductivity of the film: as the thickness increases the conductivity increased (i.e. resistivity decrease).

The dependence of resistivity or any other transport parameter on the thickness of the film is referred to as the size effect or the dimensional effect.

The activation energy for conduction decreases with increasing thickness. This decrease in activation energy in the case of thicker films may be attributed to greater deposition which builds up a more homogeneous network, thus minimizing the number of defects; these results are given in Table II.

The variation of transmission, T, of Sb_2Te_3 films deposited on amorphous substrate with wavelength λ is shown in Fig. 4. The transmittance decreases as the thickness increases. It was observed that there is a peak in the spectrum which does not vary with changing thickness. This peak may be attributed to an indirect transition, the energy of which is 1.9 eV.

The processes of nucleation and growth of thin films have been of considerable interest in studies of physical properties of materials and in studies of applications of these properties to practical advantage. The details of nucleation and growth depend on the material being deposited and on parameters such as substrate material temperature, the rate of deposition and the angle of incidence of the evaporant on to the substrate [9]. In general, when a film is deposited on a glass-like

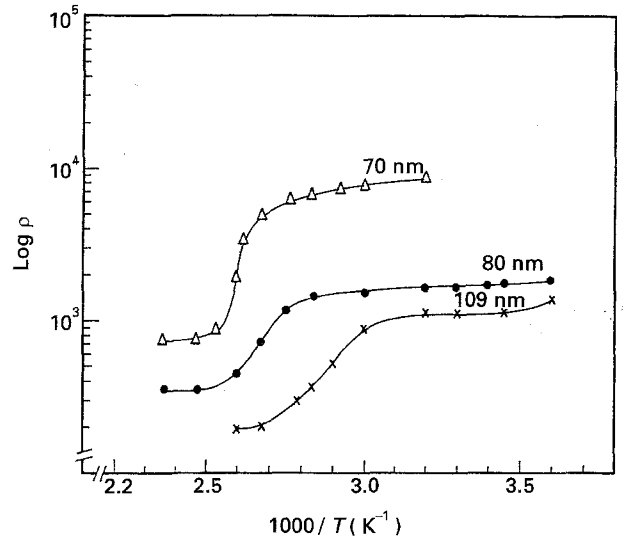

Figure 2 Log ρ versus $1/T$ plots for as-deposited Sb_2Te_3 thin films of different thicknesses.

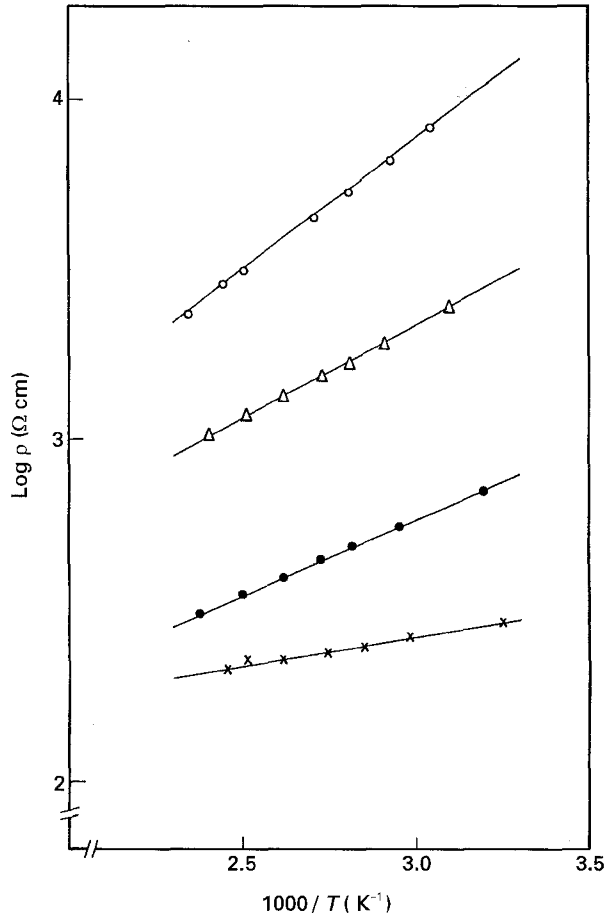

Figure 3 A plot of log ρ and $1000/T$ for annealed films of Sb_2Te_3 of different thicknesses, t: (○) 50 nm, (△) 70 nm, (●) 80 nm, (×) 109 nm.

TABLE II Activation energy of Sb_2Te_3 thin films of different thickness

Film thickness (nm)	Activation energy (eV)
50	0.071
70	0.050
80	0.040
109	0.016

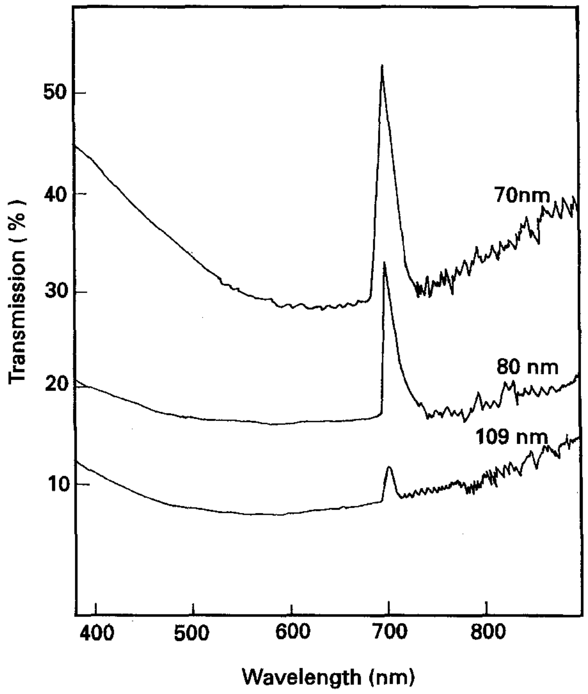

Figure 4 Relation between wavelength and transmission, T, for different thicknesses of Sb_2Te_3.

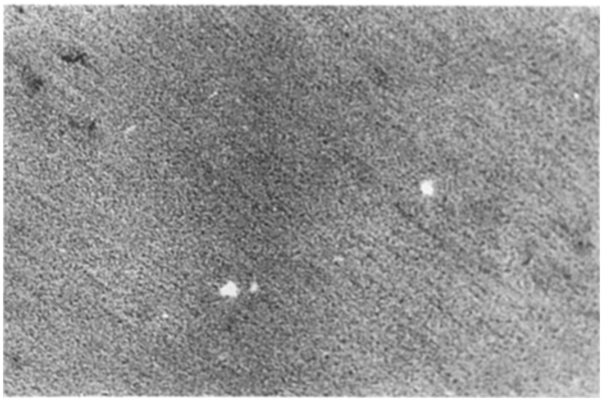

Figure 5 Electron micrograph of Sb_2Te_3 thin films deposited on quartz, thickness 50 nm × 20 000.

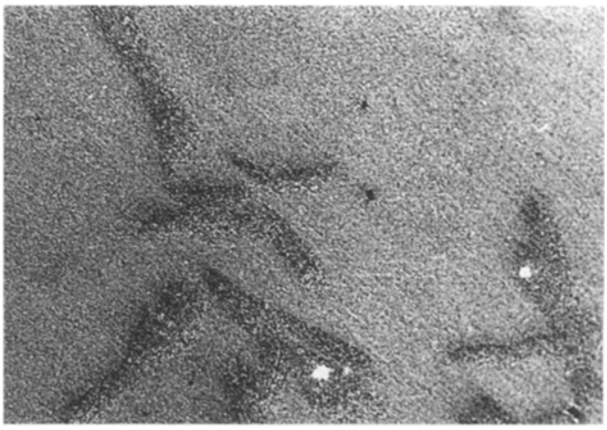

Figure 6 Electron micrograph of Sb_2Te_3 thin films of thickness 60 nm × 20 000.

substrate in vacuum by evaporation or sputtering, the nucleation of the deposited film begins at many different nucleation sites, usually at imperfections in the substrate surfaces as a result of the loss of the high mobility of particles arriving at such sites. These crystallites are usually three-dimensional even when the film thickness, as calculated from the volume of evaporated metal, is less than a monolayer [10].

Additional particles arriving from the source agglomerate about the nuclei, and an island structure is formed. As the deposition continues, islands coalesce decreasing the island density. The islands then grow until contact is made with neighbours, and gradually the voids between the agglomerates are filled, producing a filament-like network. Eventually a macroscopically uniform thin film is obtained.

Fig. 5 shows electron micrographs of the early growth of Sb_2Te_3 particles while Fig. 6 shows that the particles grow in size and coalescence between particles takes place.

This material requires more work to be undertaken on it because there is little information available in the literature.

References

1. E. J. TICHOVOLSKY and J. G. MAVROIDES, *Solid State Commun.* 7 (1969) 927.
2. L. ESAKI and P. I. STILES, *Phys. Rev. Lett.* **16** (1966) 574.
3. M. NODA, L. CHOW and K. C. KAO, *J. Phys. D* **12** (1979) 1345.
4. V. D. DASS and P. J. LAKSHMI, *J. Appl. Phys.* **62** (1987) 2376.
5. P. LOSTAK, Z. STARY, J. HORAK and J. PANCIR, *Phys. Status Solidi (a)* **115** (1989) 87.
6. B. THOMAS and T. R. N. KUTTY, *ibid.* **119** (1990) 127.
7. N. DHIREN SINGH and H. N. K. SARMA, *ibid.* **112** (1989) K 101.
8. D. W. PASHELY, *Adv. Phys.* **5** (1959) 173.
9. J. P. HIRTH and K. L. MOAZED, in "Physics of Thin Films", edited by G. Hass and R. E. Thun, Vol. 4 (Academic Press, New York, 1967) p. 97.
10. G. A. BASSETT, J. W. MENTER and D. W. PASHLEY, in "Structure and Properties of Thin Films", edited by C. Neugebauer, J. B. Newkirk and D. A. Verinclyea (Wiley, New York, 1959) p. 11.

Received 7 January
and accepted 5 September 1994